

Nanodome improved resistive switching memory performance using IrO_x nano-dots embedded in AlO_x film

W. Banerjee and S. Maikap*

Thin Film Nano Tech. Lab., Department of Electronic Engineering, Chang Gung University, Tao-Yuan 333, Taiwan,
*Corresponding Author: Tel: 886-3-2118800 ext. 5785 Fax: 886-3-2118507 E-mail: sidhu@mail.cgu.edu.tw

1. Introduction

Due to the superior performance over the conventional floating gate memory, resistive random access memory (ReRAM) devices in the form of metal-insulator-metal (MIM) structure are best choice for the next generation non-volatile memory (NVM) application. Drastically variable switching parameters, non-uniformity in switching cycles and device reliability are the biggest issues towards the adoption of ReRAM devices. Several high- κ materials and nanocrystals have been studied by researchers to fulfill those requirements [1-6]. To control the filament formation in the resistive memory devices, Cu nanocrystals on Pt electrode have been also introduced [6]. In our previous study, resistive switching memory using high- κ AlO_x film [2, 4] and IrO_x nano-dots [5] based ReRAM devices have been reported. However, the bottom electrode (BE) surface roughness as well as self assembled nanodome on the BE has a huge impact on device performance, which has not reported yet. The goal of this present work is to fabricate an electroforming free, highly efficient cross-point ReRAM devices on W-nanodome using $\text{IrO}_x/\text{AlO}_x/\text{IrO}_x(\text{ND})/\text{AlO}_x/\text{W}$ structure. Improved resistive switching at a low current compliance (I_{CC}) of $30\mu\text{A}$, high temperature (85°C) retention with stabilized multi level data storage have been observed by W-nanodome based cross-point ReRAM devices.

2. Experiment

RCA cleaned wafer went through a horizontal high-temperature furnace to grow a 200nm-thick SiO_2 on it. Sputtering system was used to deposit a 150nm-thick W layer. Photolithography and etching were the key process to have a W flat surface and self assembled W-nanodome as the BE. After that, high- κ AlO_x , IrO_x nano-dots (NDs), high- κ AlO_x and top electrode (TE) i.e IrO_x metal layer (200nm-thick) were deposited on the PR coated patterned wafer. Finally, lift-off was performed to obtain the cross-point memory devices. Fabricated $\text{IrO}_x/\text{AlO}_x/\text{IrO}_x(\text{ND})/\text{AlO}_x/\text{W}$ structure one with W-flat surface (S1) and other with self-assembled W-nanodome surface (S2), based cross-point ReRAM devices with a size of $1.5 \times 1.5\mu\text{m}^2$ were fabricated for the physical and electrical characterizations.

3. Results and discussion

Fig.1(a) shows cross-sectional high resolution transmission electron microscopic (HRTEM) image of the S2 ReRAM device. The thicknesses of the high- κ AlO_x , IrO_x , and high- κ AlO_x films are found to be ~ 5 , ~ 2 , and ~ 3 nm, respectively. W-nanodome can be observed very clearly on the surface of the BE. The base diameter of the single nanodome is ~ 8 nm with a top diameter is ~ 3 nm. The electrical performance of the devices can be drastically improved by W-nanodome, which have been discussed latter. All layers of the fabricated cross-point devices are confirmed by EDX [Fig. 1(b)]. Fig. 2(a) shows the plane view TEM images of the fabricated IrO_x NDs in the cross-point ReRAM devices. The average size and density of the NDs are found to be ~ 1.5 nm and $>1 \times 10^{13}/\text{cm}^2$, respectively. Well crystalline nature can be observed for the single IrO_x NDs [Fig. 2(b)]. The core-shell structure of the single ND is shown in Fig. 2(c). Inner core region is metallic Ir-rich and outside shell region is oxygen-rich. The IrO_x NDs are also playing an important role for the excellent electrical performance. Fig. 3(a) shows a current-voltage (I-V) hysteresis switching for the S1 devices. The initial forming voltage is $\sim 7.0\text{V}$ with a high current compliance (I_{CC}) of $500\mu\text{A}$. After 500 consecutive cycles, the ratio of high resistance state (HRS) to low resistance state

(LRS) becomes ~ 30 . The W-flat BE devices are capable to show resistive switching with a higher I_{CC} level, but not useful at the low current compliance levels ($<500\mu\text{A}$). Furthermore the switching stability can be improved by introducing W-nanodome on the BE surface [Fig. 3(b)]. No extra formation process is needed for the S2 devices, due to the presence of the W-nanodome and the poor quality of the active film, and the defects are in percolation length. This is also advantage to obtain formation free resistive switching memory. S2 devices are capable to show consecutive 10^3 DC hysteresis switching cycles at $200\mu\text{A}$ whereas S1 devices are unable to show any hysteresis at the same I_{CC} . A large resistance ratio of >100 is achievable after 10^3 DC cycles for the S2 devices. Fig. 4 shows the very tight distribution of the SET and RESET voltage with device-to-device (D/D) variation for the S1 and S2 ReRAM devices. The SET/RESET voltages are $+2.4\text{V}/-1.9\text{V}$ and $+1.1\text{V}/-0.9\text{V}$ for S1 and S2, respectively. Due to the presence of the W-nanodome, tight distributions of the SET/RESET voltages are achieved for the S2 devices. Fig. 5 shows the schematic switching mechanism. W-nanodome will concentrate the electric field on the nanodome tip as well as repeatable switching cycles. The presences of the nanodome also have been confirmed by the tapping mode atomic force microscopic (AFM) image (Fig. 6). The average surface roughness is ~ 1 nm for the S1 and ~ 8 nm for the S2 devices. The grains can be observed with a several numbers of small nanodomains with a base diameter variation from ~ 10 nm to 30 nm. The nanodome diameter is similar to the diameter found in HRTEM image. The statistical analysis of the S2 devices at $200\mu\text{A}$ and $30\mu\text{A}$ is shown in Fig. 7. The S2 device shows $\sim 98\%$ of yield. It indicates that the fabricated cross-point resistive switching memories are suitable for the multi-level data storage (MLC) application. Fig. 8 shows endurance characteristic of the S1 and S2 devices. The I_{CC} was maintained at $500\mu\text{A}$ and $200\mu\text{A}$ for the S1 and S2 devices, respectively. Poor cycle ability of 10^3 can be observed for the S1 devices owing to the smooth W surface. Whereas excellent AC cycles of $>10^5$ is observed for the S2 devices, due to the presence of the W-nanodome. Excellent retention characteristic with a stable resistance ratio at low current compliance of $30\mu\text{A}$ is shown (Fig. 12). At I_{CC} of $200\mu\text{A}$, a resistance ratio of >100 and >50 after 10^4 s of retention time are also observed at RT and 85°C , respectively. Improved self-assembled W-nanodome based formation free cross-point ReRAM device performance can be useful in future nanoscale nonvolatile memory applications.

4. Conclusion

Novel W-nanodome based $\text{IrO}_x/\text{AlO}_x/\text{IrO}_x(\text{ND})/\text{AlO}_x/\text{W}$ cross-point architecture with excellent HRS to LRS switching stability, lower operating voltage ($\pm 2\text{V}$) and current ($<30\mu\text{A}$) with data retention at 85°C is reported. Excellent AC endurance of 10^5 cycles with multi-level operation is also obtained. This W-nanodome based crossbar ReRAM device can be useful in future nanoscale (<20 nm) high-density 3D memory applications.

Acknowledgments

Thanks a lot to National Science Council (NSC), Taiwan, under contract no. NSC-97-2221-E-182-051-MY3 to support this project.

References

- [1] A. Sawa, Mater. Today, vol. 11, p. 28, 2008. [2] W. Banerjee et. al., Jpn. J. Appl. Phys, vol. 51, 04DD10, 2012. [3] H. Y. Lee et. al., IEEE Trans. Electron Dev., vol. 31, no. 1, p. 44, 2010. [4] D. S. Jeong et. al., Solid-State Electronics, vol. 63, 2011. [5] W. Banerjee et. al, Nanoscale Research Letters, vol. 7:194, 2012. [6] Q. Liu et. al., ACS Nano, vol. 4, no. 10, p. 6162, 2010.

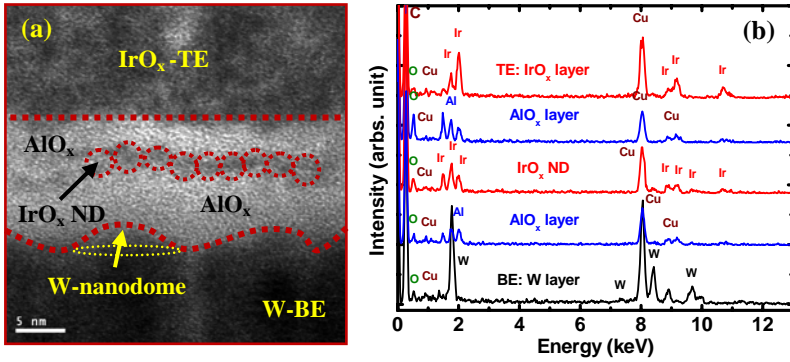


Fig. 1(a) XTEM image of an IrO_x/AlO_x/IrO_x(ND)/AlO_x/W-nanodome ReRAM cross-point memory device. (b) Energy dispersive x-ray spectra (EDX) on the IrO_x, AlO_x, IrO_x, AlO_x and W layers.

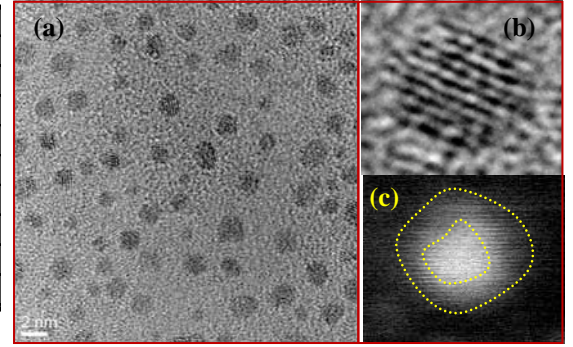


Fig. 2 (a) plane-view TEM of IrO_x NDs, (b) good crystalline single ND with (c) STEM image of single core-shell IrO_x ND of as-deposited structure.

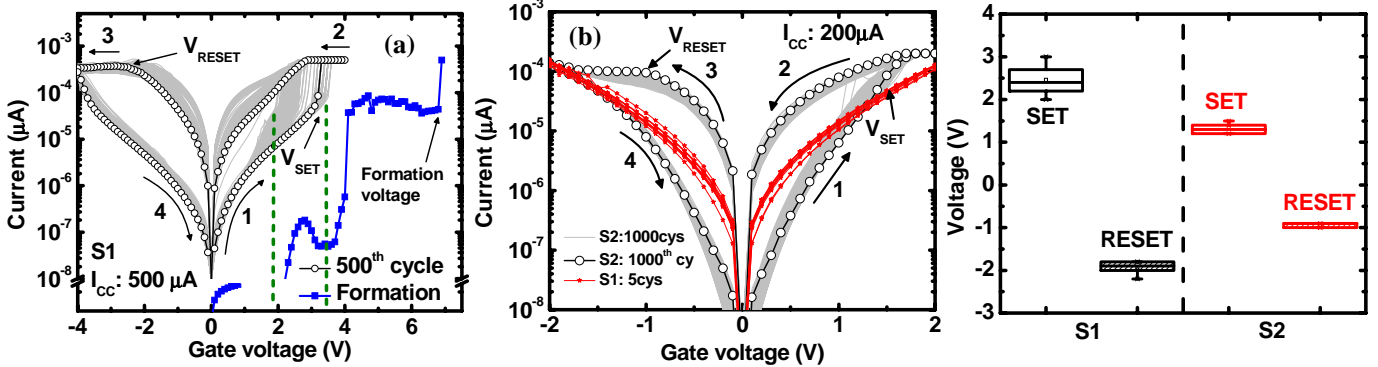


Fig. 3. (a) Initial formation process required to get switching in S1 devices. The switching direction is from 0V → 4.0V → 0V → -4.0V → 0V. (b) Formation free excellent resistive sweepings of W-nanodome devices (S2) at 200 μA. Very stable SET/RESET is observed.

Fig. 4. Tight distributions for the SET/RESET voltages of ±1V for the S2 devices are observed as compare to the S1 devices.

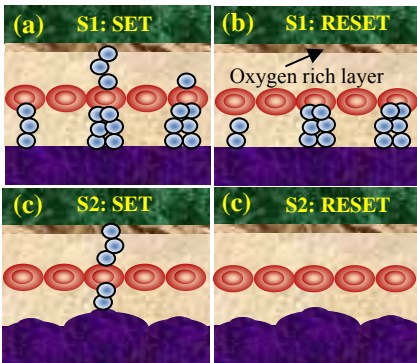


Fig. 5. Schematic views of the resistive switching mechanisms of the (a) SET, (b) RESET process for S1, and (c) SET and (d) RESET process for S2 devices are shown. The enhanced electric field on the surface of the W-nanodome will guide the oxygen vacancy nano-filament in the S2 devices.

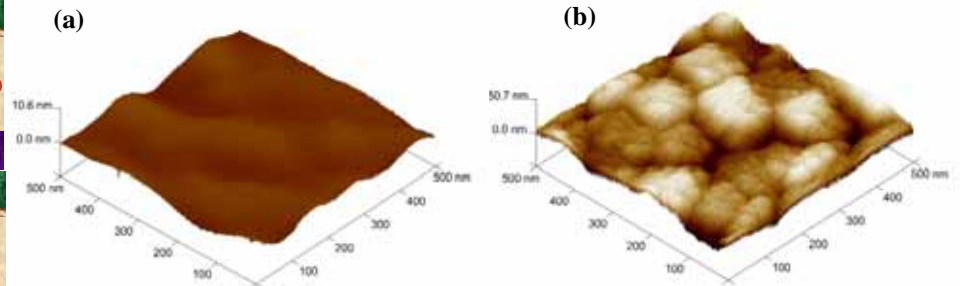


Fig. 6. AFM images of (a) W-flat surface with roughness of 1nm and (b) W-nanodome with roughness of 8nm.

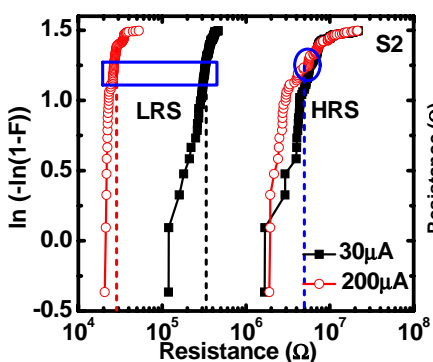


Fig. 7. Weibull distribution of the S2 devices at the I_{cc} values of 200 μA and 30 μA. Different resistances at the low resistance state show the MLC capability.

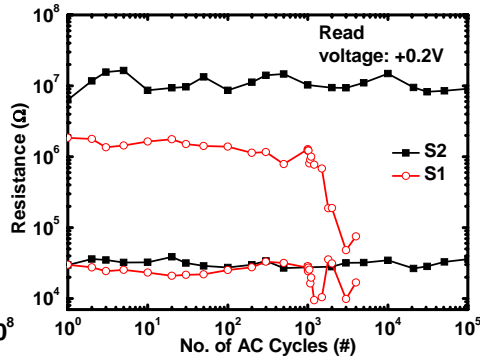


Fig. 8. Good endurance characteristics are obtained for the S2 devices as compare to the S1 devices. Improved performance is observed owing to the nano-filament through the IrO_x ND embedded in AlO_x on the W-nanodome.

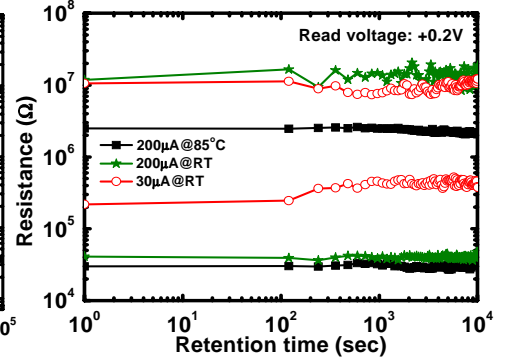


Fig. 9. Applicable resistance ratio of >50@ 85°C is achieved for the nanodome devices which shows the promise in future nanoscale 3D nonvolatile memory applications.